

## Supplementary

### Terms used for searching in databases and literature:

'DCTN1 gene', 'dynactin subunit 1', 'Perry syndrome', 'NM\_004082:c.212G>A', 'p.Gly71Glu'

### References for the supplementary tables

1. Yamada H, Neshige S, Morino H and Maruyama H: Extubation failure due to atypical parkinsonism with negligible motor and variable non-motor symptoms associated with a variant of DCTN1. *Intern Emerg Med* 18: 329-331, 2023.
2. Krishnan P, Sarma GRK, Murgod U, Srinivas M and Roy AK: Perry syndrome with a novel mutation and a rare presentation: first report from india. *Ann Indian Acad Neurol* 25: 703-706, 2022.
3. Araki E, Tsuboi Y, Daechsel J, Milnerwood A, Vilarino-Guell C, Fujii N, Mishima T, Oka T, Hara H, Fukae J and Farrer MJ: A novel DCTN1 mutation with late-onset parkinsonism and frontotemporal atrophy. *Mov Disord* 29: 1201-1204, 2014.
4. Honda H, Sasagasako N, Shen C, Shijo M, Hamasaki H, Suzuki SO, Tsuboi Y, Fujii N and Iwaki T: DCTN1 F52L mutation case of Perry syndrome with progressive supranuclear palsy-like tauopathy. *Parkinsonism Relat Disord* 51: 105-110, 2018.
5. Barreto RD, Rodrigues R, Roriz JM, Alonso I and Magalhães M: Perry syndrome with progressive supranuclear palsy-like phenotype in a Portuguese family-Long-term clinical follow-up. *Parkinsonism Relat Disord* 84: 74-76, 2021.
6. Aji BM, Medley G, O'Driscoll K, Larner AJ and Alusi SH: Perry syndrome: A disorder to consider in the differential diagnosis of Parkinsonism. *J Neurol Sci* 330: 117-118, 2013.
7. Chung EJ, Hwang JH, Lee MJ, Hong JH, Ji KH, Yoo WK, Kim SJ, Song HK, Lee CS, Lee MS and Kim YJ: Expansion of the clinicopathological and mutational spectrum of Perry syndrome. *Parkinsonism Relat Disord* 20: 388-393, 2014.
8. Silva E, Itzcovich T, Niikado M, Caride A, Fernández E, Vázquez JC, Romorini L, Marazita M, Sevelever G, Martinetto H and Surace EI: Perry disease in an Argentine family due to the DCTN1 p.G67D variant. *Parkinsonism Relat Disord* 97: 63-64, 2022.
9. Mishima T, Fujioka S, Nishioka K, Li Y, Sato K, Houzen H, Yabe I, Shiomi K, Eriguchi M, Hara H, *et al*: Meta-iodobenzylguanidine myocardial scintigraphy in Perry disease. *Parkinsonism Relat Disord* 83: 49-53, 2021.
10. Farrer MJ, Hulihan MM, Kachergus JM, Dächsel JC, Stoessel AJ, Grantier LL, Calne S, Calne DB, Lechevalier B, Chapon F, *et al*: DCTN1 mutations in Perry syndrome. *Nat Genet* 41: 163-165, 2009.
11. Stoker TB, Dostal V, Cochius J, Williams-Gray CH, Scherzer CR, Wang J, Liu G and Coyle-Gilchrist I: DCTN1 mutation associated parkinsonism: Case series of three new families with perry syndrome. *J Neurol* 269: 6667-6672, 2022.
12. Milanowski L, Sitek EJ, Dulski J, Cerquera-Cleves C, Gomez JD, Brockhuis B, Schinwelski M, Kluj-Kozłowska K, Ross OA, Sławek J and Wszolek ZK: Cognitive and behavioral profile of Perry syndrome in two families. *Parkinsonism Relat Disord* 77: 114-120, 2020.
13. Caroppo P, Le Ber I, Clot F, Rivaud-Péchéoux S, Camuzat A, De Septenville A, Boutoleau-Bretonnière C, Mourlon V, Sauvée M, Lebouvier T, *et al*: DCTN1 mutation analysis in families with progressive supranuclear palsy-like phenotypes. *JAMA Neurol* 71: 208-215, 2014.
14. Konno T, Ross OA, Teive HAG, Sławek J, Dickson DW and Wszolek ZK: DCTN1-related neurodegeneration: Perry syndrome and beyond. *Parkinsonism Relat Disord* 41: 14-24, 2017.
15. Tacik P, Fiesel FC, Fujioka S, Ross OA, Pretelt F, Castañeda Cardona C, Kidd A, Hlavac M, Raizis A, Okun MS, *et al*: Three families with Perry syndrome from distinct parts of the world. *Parkinsonism Relat Disord* 20: 884-888, 2014.
16. Newsway V, Fish M, Rohrer JD, Majounie E, Williams N, Hack M, Warren JD and Morris HR: Perry syndrome due to the DCTN1 G71R mutation: a distinctive levodopa responsive disorder with behavioral syndrome, vertical gaze palsy, and respiratory failure. *Mov Disord* 25: 767-770, 2010.
17. Boardman J, Mascareno Ponte M, Chaouch A and Kobylecki C: Perry syndrome with intrafamilial heterogeneity in presentation and survival including acute respiratory failure: Case series. *Mov Disord Clin Pract* 9: 816-820, 2022.
18. McManus EJ, Poke G, Phillips MC and Asztely F: Perry syndrome: A case of atypical parkinsonism with confirmed DCTN1 mutation. *N Z Med J* 133: 116-118, 2020.
19. Čierny M, Hooshmand SI, Fee D, Tripathi S, Dsouza NR, La Pean Kirschner A, Zimmermann MT and Brennan R: Novel destabilizing Dynactin variant (DCTN1 p.Tyr78His) in patient with Perry syndrome. *Parkinsonism Relat Disord* 77: 110-113, 2020.
20. Lechevalier B, Chapon F, Defer G, Rivrain Y, Le Doze F, Schupp C and Viader F: Perry and Purdy's syndrome (familial and fatal parkinsonism with hypoventilation and athymhormia). *Bull Acad Natl Med* 189: 481-490; discussion 490-2, 2005 (In French).
21. Purdy A, Hahn A, Barnett HJ, Bratty P, Ahmad D, Lloyd KG, McGeer EG and Perry TL: Familial fatal Parkinsonism with alveolar hypoventilation and mental depression. *Ann Neurol* 6: 523-531, 1979.

Figure S1. Spatial relationship of the residue at position 71 of the CAP-Gly domain. Images show the residues located spatially close (4 Å) to Gly71 in the wild-type CAP-Gly domain (left) and the equivalent representation of residues close to Glu71 in the mutant models (right). Gly71 and Glu71 are represented as blue and red spheres (2MPX/Model 3), respectively, or by element (2HKQ/Model 2 and 3E2U/Model 4). In 2MPX/Model 3, the residues in the proximity of position 71 are shown as green spheres. The remaining images are shown in the stick format. The remaining regions of the molecules are represented in cartoon format. The residues of interest are identified using the one letter code. In Model 2, Glu71 is oriented in the opposite direction compared with Model 1 shown in Fig. 1C. Glu71 points toward the  $\beta$ 3 strand, which is part of the structural core of the domain. Consequently, both Phe79 and Cys81 rearrange to create room for Glu71. In Model 3, Glu71 is oriented towards the domain surface, as in Model 1, but it is more solvent-exposed in Model 3. Such variation in the environment of Glu71 reflects differences in the loop conformation connecting the  $\beta$ 3 and  $\beta$ 4 strands between these models, resulting in a less compact environment of Glu71 in Model 3. In Model 4, Glu71 adopts a spatial positioning similar to that adopted in Model 2, but in Model 4, the Glu71 side chain is rotated nearly 90°, respective to Model 2. Å, Angstrom; CAP-Gly, cytoskeleton-associated protein glycine-rich domain; 2MPX, three-dimensional structure of cap-gly domain assembled on microtubules determined by Magic Angle Spinning NMR spectroscopy; 2HKQ, crystal structure of the C-terminal domain of human EB1 in complex with the CAP-Gly domain of human dynactin-1 (p150-Glued); 3E2U, crystal structure of the zink-knuckle 2 domain of human CLIP-170 in complex with p150-Glued.

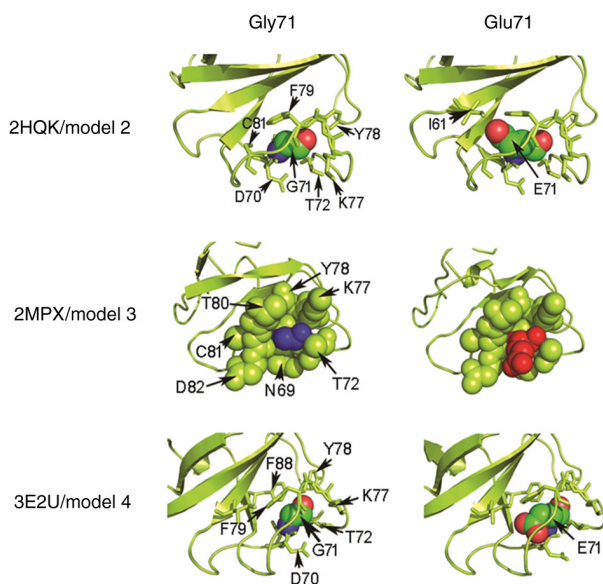


Figure S2. Cavities in the structures of the 2HKQ/Model 2, 2MPX/Model 3 and 3E2U/Model 4. The analysis was performed using the Voronoia program suite (21). The cavities are represented as spheres with mesh format, in blue or green. In the protein structures, the peptide backbone is shown in the cartoon format and the lines indicate residues, except position 71 (Gly or Glu), which is shown as a sphere. The image was generated by PyMOL (20) using data in the cav PDB file generated by Voronoia and the PDB file of respective structures. PDB, protein data bank; 2HKQ, crystal structure of the C-terminal domain of human EB1 in complex with the CAP-Gly domain of human dynactin-1 (p150-Glued); 2MPX, three-dimensional structure of cap-gly domain assembled on microtubules determined by Magic Angle Spinning NMR spectroscopy; 3E2U, crystal structure of the zink-knuckle 2 domain of human CLIP-170 in complex with p150-Glued PDB entries.

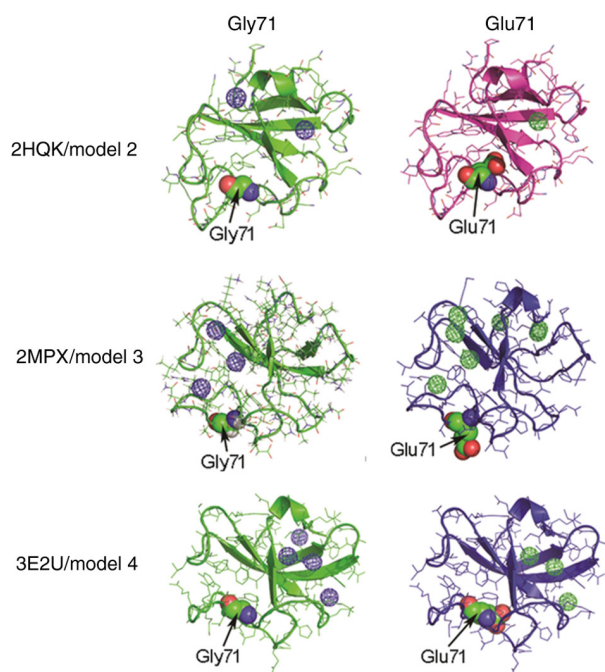


Figure S3. Electrostatic potential maps of the 2HKQ/Model 2, 2MPX/Model 3 and 3E2U/Model 4 protein structures, constructed using Swiss-PdbViewer 4-1-0 software (22). The conventional code represents the charge distribution, where blue and red represent electron-poor and electron-rich regions, respectively. The molecules are represented in a space-filled format, using the CPK color code: Carbon is gray, oxygen is red, nitrogen is blue, sulfur is yellow and hydrogen is white. 2HKQ, crystal structure of the C-terminal domain of human EB1 in complex with the CAP-Gly domain of human dynactin-1 (p150-Glued); 2MPX, three-dimensional structure of cap-gly domain assembled on microtubules determined by Magic Angle Spinning NMR spectroscopy; 3E2U, crystal structure of the zink-knuckle 2 domain of human CLIP-170 in complex with p150-Glued; CPK, Corey-Pauling-Koltun.

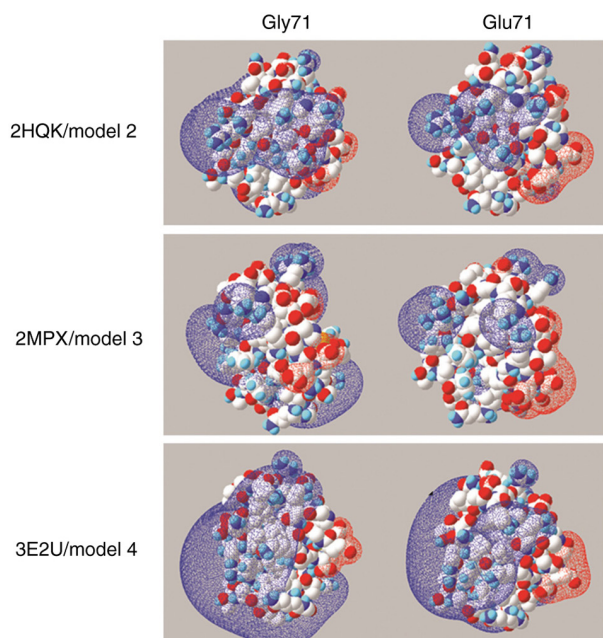


Figure S4. (A) Prediction of aggregation/amyloidogenic-prone sequences in the CAP-Gly domain of p150glued protein. The analysis was performed using the web-based tool AmylPred2, a consensus method for predicting amyloid propensity (21). Consensus-5 indicates that the sequence was predicted to be prone to aggregate as amyloid by at least 5 of the 10 algorithms applied by AmylPred2. The three segments identified as consensus-5 are highlighted in dark blue, red and light gray in the CAP-Gly domain sequence. The pattern of secondary structure elements in the protein is shown at the top. The regions folded as  $\beta$  strands are represented as arrows and the short helix near the C-terminus is represented as a short cylinder. The downward red and blue arrows indicate the Gly59 and Gly71 residues, respectively. The conserved GKNDG motif is highlighted with a black bar. The result of each algorithm is shown below consensus-5. (B) Location of the consensus-5 sequences identified by AmylPred2 analysis in the CAP-Gly domain of p150glued protein. The regions are shown in the same color pattern as aforementioned in A. The  $\beta$ -strands 1-4 and Gly59 and Gly71 residues are indicated by arrows. The image on the right side is rotated 180°, respective to the left image. Graphical images were generated by PyMOL (20) using the coordinates contained in protein data bank no. 3E2U. CAP-Gly, cytoskeleton-associated protein glycine-rich domain; GKNDG motif, Glycine-Lysine-Asparagine-Aspartic acid-Glycine motif; Amyl Patt, amyloidogenic pattern; Av P Densit, average packing density;  $\beta$ -str Cont,  $\beta$ -strand contiguity; Hexa C Ener, hexapeptide configuration energy; N-term, N-terminus; C-term, C-terminus.

